Applied Numerical Modeling in Geomechanics – 2020 – Billaux, Hazzard, Nelson & Schöpfer (eds.) Paper: 08-01

Distinct Element Method (DEM) for fibrous composites: Toward computational guided manufacturing

Traian Dumitrică[1], Yuezhou Wang[2], Hao Xu[3], Grigorii Drozdov[4] & Igor Ostanin[5,6]
[1]*Department of Mechanical Engineering, University of Minnesota, Minneapolis, MN, USA*
[2]*Department of Integrated Engineering, Minnesota State University, Mankato, MN, USA*
[3]*Department of Aerospace Engineering and Mechanics, University of Minnesota, Minneapolis, MN, USA*
[4]*Scientific Computing Program, University of Minnesota, Minneapolis, MN, USA*
[5]*Skolkovo Institute of Science and Technology, Nobel St. 3, Moscow, Russia*
[6]*University of Twente, Enschede, The Netherlands*

1 INTRODUCTION

DEM (Cundall & Strack 1979) is a model proposed 40 years ago in the Department of Civil, Environmental, and Geo-Engineering at University of Minnesota. The method is based on the use of a numerical scheme in which the interaction of the particles is monitored contact-by-contact, and the motion of the particles modeled particle-by-particle. DEM endured the test of time. Today, the model is successfully used in geotechnical, earth sciences, fluids, and pharmaceutical simulations

We are exploring the new application of DEM to fibrous composites (FCs). In general, manufacturing of FCs (such as carbon fiber reinforced polymers, carbon nanotube polymer composites, textiles made from active fibers) is subject to substantial challenges, which are mainly caused by the discontinuities of the fibers. In this respect, it is inspiring to know that the most performant structures in Nature exhibit discontinuous architectures at various length of scale (Zhao et al. 2018). These architectures are able to combine the benefits of strength and stiffness with outstanding toughness and damage tolerance. For FCs, the optimal discontinuous fiber architecture are not known, but can be proposed by advanced DEM computations.

DEM for FCs, or mesoscopic DEM, has the potential to advance the manufacturing of FC structures. Since an exhaustive exploration of the large parameter space (fiber length, fiber diameter, filler material etc.) by direct manufacturing of FCs is impractical, the guidance offered by mesoscopic DEM is critical. Here we address simulations for guiding the manufacturing of ultra-strong carbon nanotube (CNT) composites. During synthesis, the parameters (diameter, length, number of inner walls) of the individual CNTs can be adjusted, but the consequences on the materials' properties are not known a priori. mesoscopic DEM simulations are used to predict the variations in mechanical response caused by these parameters, and to guide the synthesis conditions toward the optimal parameters of the CNTs.

Here we focus on the complex stretching process of CNT mats that involves subtle microstructural evolution, including de-bundling, waviness, zipping, etc. The factors that most decisively impacts the transition from the rather stochastic network structure to the yarn structure are not well understood. With the help of mesoscopic DEM, we simulate the stretching of various networks consisting of several hundred CNTs. Aiming at engineering highly aligned CNT yarns with reduced porosity, we explore by mesoscale simulations the impact of CNT length, friction, entanglement and bundling, and identify the significant contributing factors to the yarn formation. Most work presented in this abstract has been published in the references (Wang et al. 2015, Wang et al. 2018).

2 DESIGN AND ANALYSIS

Mesoscopic DEM is a coarse-grained representation of the system in question as each element generally represents a segment of the detailed CNT containing many carbon atoms. Specifically, we have discretized

a (10,10) single-walled CNT such that each cylindrical tubule discrete element of length of 1.36 nm, radius 0.68 nm, and thickness 0.335 nm represents 220 carbon atoms of the underlying atomistic system (Fig. 1a). These mesoscopic elements are tracked in the Lagrangian frame. In the PFC implementation, they are evolved deterministically in time as rigid bodies with a damped scheme based on a velocity Verlet algorithm for translations and a fourth-order Runge-Kutta for rotations. The time step used in the mDEM simulations is 30 fs.

The interactions between elements are described through standard parallel-bonds and newly designed van der Waals (vdW) contact bonds. Parallel-bond contacts were trained (Ostanin et al. 2013) to capture the intratube covalent interactions responsible for the local linear elasticity of individual CNTs, including stretching, shearing, bending and torsion, resembling the behavior of classical Euler-Bernoulli beam (Fig. 1b). The cylindrical distinct elements are connected by parallel-bond contacts, which introduce normal and shear forces ($\boldsymbol{F_n}$ and $\boldsymbol{F_s}$) and moments ($\boldsymbol{M_n}$ and $\boldsymbol{M_s}$) to resist relative displacements and rotations.

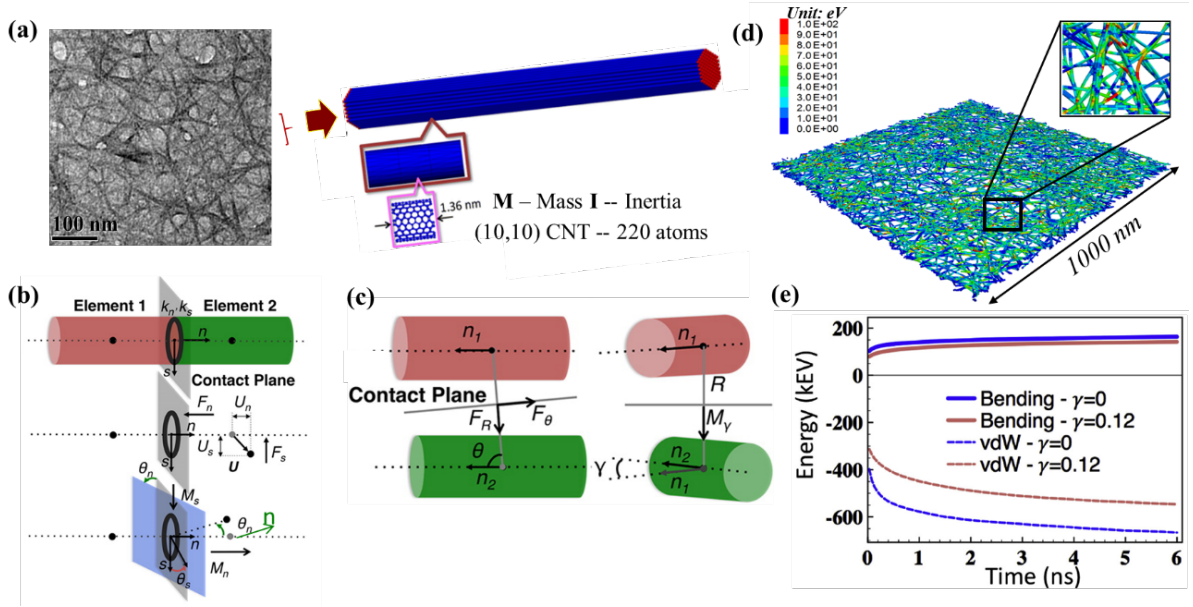

Figure 1. (a) Transmission electron microscopic picture of CNT network. The fibers are discretized and modeled as a chain of rigid distinct element in cylindrical shape. (b) Parallel-bond contact mode. (c) vdW contact model. (d) mDEM representation of a CNT network. (e) Energies evolution during the relaxation process of the network in (d) with and without nanofriction.

Distinct elements located on two different CNTs may interact via vdW contacts (Fig. 1c). The vdW contact has been developed by us via a procedure that involves the integration of the atomistic vdW interactions between two CNTs (Ostanin 2013). Our vdW contacts capture the general case when two finite size CNTs are misaligned and crossed. Unlike isotropic potentials our anisotropic vdW potential is free of "corrugated" spurious effects (Volkov et al. 2010), which could cause artificial load transfer between CNTs. Thus, in mesoscopic DEM misaligned (shifted) parallel CNTs will undergo smooth sliding under the action of mesoscopic vdW forces. Similarly, crossed CNTs will be zipping under the action of the long-ranged vdW forces and aligning moments. Reference (Ostanin et al. 2013) gives the explicit forms for these mesoscopic forces and moments.

Another important feature is the presence of viscous damping modeled as $\boldsymbol{F_d} = \gamma \cdot \boldsymbol{v_r}$, where $\boldsymbol{F_d}$ is the friction force, $\boldsymbol{v_r}$ the relative velocity of the distinct elements in vdW contact, and γ is the linear viscous coefficient. The calibration of viscous effect is done by sliding two segments of CNT against each other and measuring the reaction forces in both mesoscopic DEM and Molecular Dynamics (MD) simulations. By choosing $\gamma = 0.12\ pN\ s/m$, mesoscopic DEM provides the equivalent nanoscale friction in agreement with MD results. Meanwhile, the same γ is tested against aligning time when two crossed CNTs align under vdW attraction.

To arrive at the structure shown in Figure 1a, we computer generated a random network of straight (strain free) CNTs, which contains 500 CNTs each 950 nm in length. The network was relaxed under vdW attraction freely for 6 ns (2×10^5 cycles). In Figure 1d and 2, the relaxed structure shows significant increase of bending energy counterbalanced by increasing the vdW cohesive energy due to zipping relaxation of CNT portions. Both the simulated density (0.14 g/cm^3) and the characteristic pore size (150 nm^2 – 200 nm^2) match the characteristics of realistic CNT aerogel materials.

3 RESULTS AND DISCUSSION

We then stretched the network up to 150% strain through displacement-controlled tensile test. The stretched network undergoes significant restructuring, with the formation of a central yarn comprising aligned CNTs, Figure 2a. To understand this remarkable process, Figure 2b shows the calculated stress-strain (ε) curve. In correspondence to the structure evolution, we have identified four distinct regimes: (i) elastic, for ε < 3%, (ii) softening, for 3% < ε < 30%, (iii) stiffening, for 30% < ε < 60%, and (iv) softening and failure, for ε > 60%.

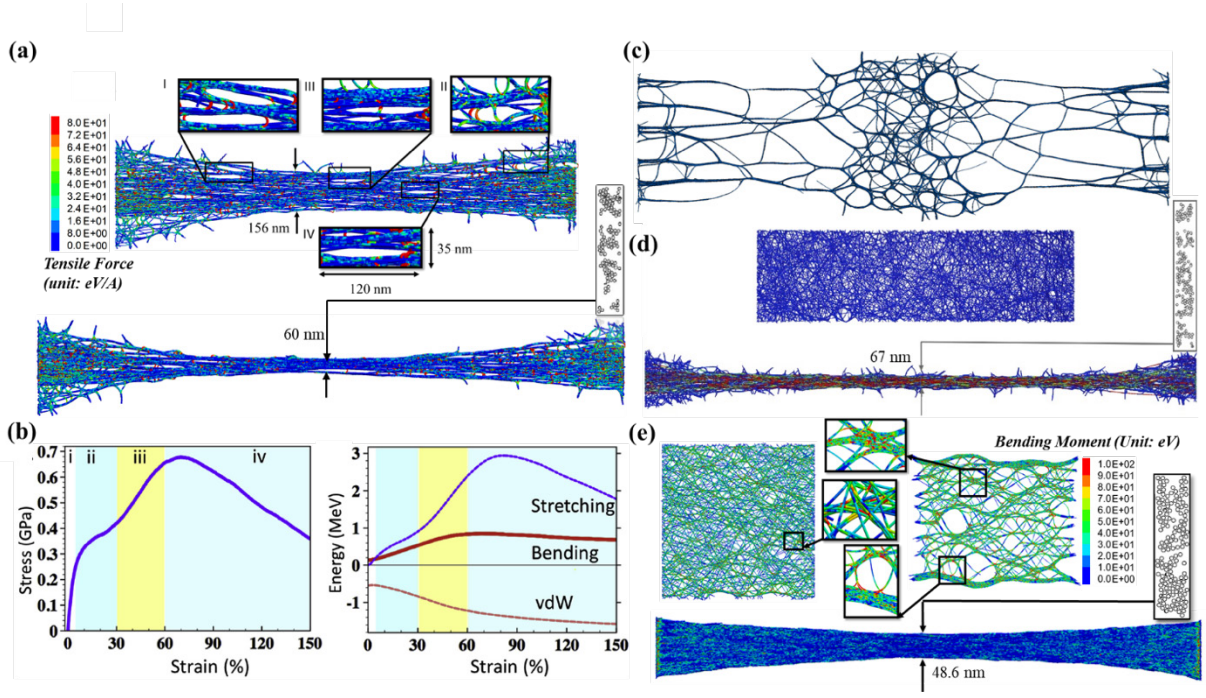

Figure 2. (a) CNT network stretched to 75% and 150% strain showing the closure of pores and packing of the yarn cross-section. (b) Strain-stress relation and energy evolution during the tensile test of (a). (c) Stretching of CNT network without nanofriction shows big pore opening. (d) A CNT ribbon stretched to 90% strain. (e) Anisotropic networks relaxed with/without friction (left/right). The network with friction is stretched to 75% strain showing a better packing at yarn's cross-section.

The elastic regime gives a Young's Modulus of 8.6 GPa. With the load transfer just begins to develop, zipping relaxation activation is limited. As stretching progresses (regime ii), the network softens significantly. The behavior can be seen in the slope changes presented by the stress-strain and stretching energy curves in Figure 2b. At the microstructure level, the local bundling and the pore sizes are increasing. Pores undergo squashing, especially in the central region of the network, under the transverse contraction caused by the Poisson's effect and the zipping relaxation directed by the strain direction. The hardening (regime iii) features energetic elasticity of wavy CNTs, visible in the evolution of the stretching energy, Figure 2b. Energetic elasticity is enabled by the increase in entanglement under pore squashing. The yarn formation also begins in this regime as alignment becomes significant. At regime iv, entangled CNTs can no longer sustain the load transfer, leading to its final softening and failure. As the stretched CNTs begin to straighten

their severely bent portions located around larger pores, the bending energy drops. Above 75% strain, the dominance of elastic deformation is substituted by inter-tube CNT sliding corresponding to the thinning of the bundle and increase in packing density. The final stage shows organization into three main aligned bundles, each containing about 30 CNTs, separated by nm size pores.

In absence of nanofriction ($\gamma = 0\ pN\ s/m$), the network (Fig. 2c) will no longer support a good load transfer, since sliding and disentanglement become much easier. Instead of promoting CNT alignment, the applied uniaxial strain accelerates the film evolution toward a cellular network, characterized by disparate bundles and large pores.

Additionally, our studies are also expanded to parametric investigations on the effect of cellular structure and anisotropy. It is noted that given a long-time scale, CNT network is slowly evolving toward a cellular network with large pores. While the computational time with mesoscopic DEM to achieve this cellular structure via relaxation may be demanding, cyclic loading that removes the kinetic barriers can accelerate the dynamics. Following this approach, we have subjected our network to six 60% compression-recovery cycles. The resulting cellular network lowered its energy by nearly 100%. During the tensile test, the stretching of these CNTs can lead to un-zipping at the microstructure level. Even with the presence of friction, the load transfer is not sufficiently potent to insure a massive bundle-to-bundle zipping relaxation directed along the applied strain direction. Therefore, the yarn presents many disparate bundles separated by large pores evolved from the original structure.

By designing a CNT ribbon 2000 nm × 500 nm × 11 nm in dimensions, CNTs are longer (814 nm) in tensile direction (Fig. 2d). The three times ($\gamma = 0.36\ pN\ s/m$) larger than the phononic friction was selected to explore the trend when dissipation is enhanced by the presence of polymeric layers between CNTs (Naraghi et al. 2010, Downes et al. 2015). During the tensile test, the formation of the yarn is significantly accelerated by the faster zipping relaxation of the nearly transversal oriented CNTs, which by construction are expected to be shorter than the 814 nm in length nearly-axial CNTs. At ε =90%, the packing and density of the yarn are enhanced in contrast to the isotropic network.

Alternatively, isotropy can also be controlled through removal of randomness, meaning the orientation of CNTs generated at initial stage is within $\pm 45°$ with respect to the tensile direction. We note that without friction, even at the relaxation stage, vdW attraction has already driven the structure into cellular formation (Fig. 2e right). The large pores will not thus be closed due to lack of sufficient load transfer as already pointed out. Nevertheless, when friction is included, the yarn formation is significant improved even at 75% strain as can be seen from the cross-sectional packing in Figure 2e.

4 CONCLUSIONS

We present DEM simulations for the mesoscale mechanical stretching of CNT networks. At small and moderate deformations, zipping relaxations along the applied strain direction dictates the microstructural evolution. At larger deformations, the occurrence of energetic elasticity promotes yarn densification, by relaxing CNT waviness and eliminating squashed pores. In addition, simulations indicate that friction and film morphology are key factors in the yarn formation: While lack of friction compromises the strain-induced alignment process, friction promotes CNT alignment by enabling load transfer and directed zipping relaxations, especially in networks containing long and entangled CNTs. In terms of morphology, we also designed anisotropic network with a preferred alignment in tensile direction. Upon stretching, such network transforms a higher quality of yarn with a better packing density. The parametric studies demonstrate friction facilitate the yarn formation, while the cellular structure (larger porosity) may play an adverse role.

We conclude by noting that the application of DEM to CNTs is an important development because it fills a gap in the available simulation methods for FCs. Indeed, finite element modeling (FEM) methods can successfully analyze the behavior at continuum scale. However, extending FEM down to the “fiber” scale is challenging due to the complex topologies, inhomogeneities, and the dynamical inter-tube sliding. Nevertheless, as the current work shows, accounting for this mesoscale is critical. The current simulations are at the basis of a “Fiber Flow” toolbox of *PFC3D* (Itasca 2018). While we are currently capturing systems

comprising a few hundred CNTs, massive parallel DEM numerical simulations (Ostanin et al. 2018) will enable us to move closer to the length and time scales required to extract representative mechanics of CNT materials.

ACKNOWLEDGEMENTS

This work was supported by University of Minnesota's MnDRIVE RSAM program, NASA's Space Technology Research Grant NNX16AE03G, the Institute for Ultra-Strong Composites by Computational Design, Grant NNX17AJ32G, and by the Fulbright U.S. Scholar program.

REFERENCES

Cundall, P.A. & Strack, O.D.L. 1979. A Discrete Model for Granular Assemblies. *Geotechnique* 29 47–65.

Downes, R.D., Wang, S., Haldane, D., Moench, A. & Liang, R. 2015. Strain-induced alignment mechanisms of carbon nanotube networks. *Adv. Eng. Mater.* 17, 349-358.

Itasca Consulting Group, Inc. 2018. *PFC3D – Particle Flow Code in Three-Dimensions, Ver. 6.0*. Minneapolis: Itasca.

Naraghi, M., Filleter, T., Moravsky, A., Locascio, M. & Loutfy, R.O., Espinosa, H.D. 2010. A multiscale study of high-performance double-walled nanotube polymer fibers. *ACS Nano* 4, 6463-6476

Ostanin, I., Ballarini, R., Potyondy, D, & Dumitrică, T. 2013. A distinct element method for large scale simulations of carbon nanotubes assemblies. *J. Mech. Phys. Solid*. 61, 762-782

Ostanin, I., Zhilyaev, P., Petrov, V., Dumitrică, T., Eibl, S., Ruede, U. & Kuzkin, V. 2018. Toward large scale modeling of carbon nanotube systems with the mesoscopic distinct element method. *Lett. Mater*.8 240-245.

Volkov, A.N. & Zhigilei, L.V. 2010. Mesoscopic interaction potential for carbon nanotubes of arbitrary length and orientation. *J. Phys. Chem.* C 114, 5513-5531.

Wang, Y., Ostanin, I., Gaidau, C. & Dumitrică, T. 2015. Twisting carbon nanotube ropes with the mesoscopic distinct element method: geometry, packing, and nanomechanics. *Langmuir* 31, 12323-12327.

Wang, Y., Xu, H., Drozdov, G. & Dumitrică, T. 2018. Mesoscopic friction and network morphology control the mechanics and processing of carbon nanotube yarns. *Carbon* 139, 94-104

Zhao, H., Yang, Z. & Guo, L. 2018. Nacre-inspired composites with different macroscopic dimensions: strategies for improved mechanical performance and applications. *NPG Asia Materials* 10, 1–22.